Journal of Engineering Science and Technology
Vol. 12, No. 7 (2017) 1804 - 1818

ON THE SOLIDIFICATION CHARACTERISTICS AND MECHANICAL PROPERTIES OF ALUMINUM ALLOY AA 6061/Al_2O_3-SiC_P COMPOSITE PRODUCED BY HIGH PRESSURE DIE CASTING

BABAFEMI MALOMO[1,*], ODUNAYO FADODUN[2], KUNLE OLUWASEGUN[3], ADEDAPO OGUNBODEDE[4], SIMEON IBITOYE[3], LABO ADEKOYA[1]

[1]Department of Mechanical Engineering, Obafemi Awolowo University,Ile-Ife, Nigeria
[2]Department of Mathematics, Obafemi Awolowo University, Ile-Ife, Nigeria
[3]Department of Materials Science & Engineering, Obafemi Awolowo University,Ile-Ife, Nigeria
[4]Department of Aeronautics and Astronautics, Kwara State University, Nigeria
*Corresponding Author: bobmalom@oauife.edu.ng

Abstract

The effectiveness of the high pressure die casting (HPDC) process in facilitating a controlled solidification mechanism during the fabrication of hybrid (Al_2O_3-SiC_p) reinforced aluminum alloy composite is investigated. The aluminum matrix composite was synthesized with 5%, 10% and 20% volume fraction of reinforcements by infiltrating molten aluminum AA 6061 via squeeze casting into prefabricated ceramic preforms. The parameters for experimentation are the casting pressure (80MPa), pouring temperature (740 ^{0}C), die preheat temperature (300 ^{0}C), pressure holding time (15 s) and die cooling rate of 0.2 kg/s water flow rate. The composites were examined by optical microscopy, mechanical properties determined by tensile testing and fractured specimens analyzed by SEM fractography. The results indicate that the sample with 5% volume fraction of reinforcements showed significant variations in temperature profile and intensities of phase transformation at the beginning and the end of solidification, while for samples with 10% and 20% volume fractions, this process occurred at fairly constant temperatures with minimal inflexions in phase characteristics. The solidification time increased progressively with increasing volume fraction of reinforcements as the cooling rates reduce, and the mechanical properties with the exception of percent elongation were enhanced with increasing volume fractions of reinforcements.

Keywords: Aluminum alloy AA 6061, HPDC, Hybrid composites, Solidification, Volume fraction of reinforcement.

Nomenclatures

bl	Baseline curve, $^0C/s$
cc	Cooling curve, $^0C/s$
$^0C/s$	Cooling rate (Fig. 6)
f_s	Solid fraction parameter (Fig. 7)
T	Alloy temperature (Fig. 5), ^{0}C
t	Solidification time, sec.
t_1	Time at the beginning of solidification, sec.
t_s	Time at the end of solidification, sec.

Greek Symbols

α	Parameter for aluminum nucleation phase

Abbreviations

ASTM	American Society of Testing Materials
CTE	Coefficient of Thermal Expansion
HPDC	High Pressure Die Casting
SEM	Scanning Electron Microscope
UTS	Ultimate Tensile Strength
YS	Yield Strength
XRD	X-ray Diffraction

1. Introduction

Presently, aluminum alloys are regarded as revolutionary materials of significant technological importance due to their excellent mechanical properties and dimensional accuracy. As a result, they are candidate materials for the development of particle-reinforced metal matrix composites, required in advanced high-strength and weight-critical applications [1, 2]. However, an important concern in the mechanical industry is the capacity to produce bulk metal matrix composites (high volume percentage of micro particles), with high structural integrity; to this effect, the high pressure die casting (HPDC) method is considered as one the most consistent economical route [3, 4]. This notwithstanding, the effect of defects resulting from cold fills, entrapped bubbles, etc., associated with HPDC imparts negatively on the quality and mechanical properties of castings. It has been reported that the mechanical properties cannot be successfully enhanced by post processing methods (i.e., heat treatment etc.); but rather, by controlled synthesis approaches based on conditions which can influence to a greater extent, the properties of alloy composition and the solidified microstructure [4]. Hence, the knowledge of the solidification characteristics is very critical in many respects [4, 5].

The mechanism of solidification can be best understood by accounting for the influence of such parameters as temperature distribution, solidification condition and alloying during solidification processing. The control of solidification parameters plays a significant role in relating solidification conditions to mechanical behavior. Recently, with respect to microstructure evolution, the cooling rate is regarded as a very important solidification parameter as it gives information on temperature fields ahead of the solid-liquid interface [6, 7]. The control of the temperature fields in the casting volume has facilitated the modifications of the eutectic silicon phase of important aluminum alloys crucial

to improvements in mechanical behaviour [6, 8]. Furthermore, mechanical properties have been related to the dendrite size in aluminum alloys and used for cooling rate inference [9]. Micro hardness and strength have also been shown to increase correspondingly with cooling rates [10]. At any rate, the cooling rate has profound effect on metallurgical integrity of aluminum castings.

Investigating the influence of cooling rates on solidification parameters during casting has been made feasible by thermal analysis techniques where, notable alloy characteristics such as, temperature variations, phase transformations, solid fractions and microstructural evolution could be evaluated closely using differential thermal, differential scanning calorimetric analysis and the computer-aided cooling curve method [11]. The solidification parameters of monolithic aluminum alloys have been studied extensively using these aforementioned methods, but presently, there is limited information regarding the solidification characteristics of two-phase material systems. It has however been reported that the influence of the variations in the thermo-physical conditions while developing composite materials are significant due to the presence and interaction of hard particles in the solidifying matrix alloy and consequently, the solidification phenomena becomes tremendously complicated [12]. There is still no acceptable general theory in this regard as the subject is still not fully understood [13].

This study however investigates the effects of variations in temperature profile at the liquid-metal/solid ceramic contacting surfaces during high pressure die casting on the solidification parameters of aluminum alloy AA 6061 reinforced with SiC_p+Al_2O_3 micro particles at varying concentrations, based on the premise that pressurized solidification can influence the heat and mass transfer condition in the melt ahead of the solid-liquid interface with significant effects on the mechanical properties [14].

2. Materials preparation and fabrication of hybrid composite

The synthesis and the production of the AA 6061 aluminum alloy composite are presented in this section.

2.1. Materials and preform development

Aluminum alloy 6061 was used as a matrix material, while alumina (Al_2O_3) and silicon carbide (SiC) particles were used as raw materials for the preparation of reinforcements. The chemical composition of the matrix and the properties of the reinforcements are shown in Tables 1 and 2. The Al_2O_3 with particle size of 20 μm and SiC particles in the range of 7-10μm were mixed in the ratio of 2:1 and blended in a high-energy ball mill for 10 hours using a 304 stainless steel ball of 12 mm in diameter. The ball to powder ratio was 10:1 and 5 wt. % paraffin wax was used as a binding agent. The resulting mixture was poured into a mould to form a prefabricated bulk ceramic (preform), oven-dried at 50 ^{0}C and sintered at over 400 ^{0}C. The porosity levels on prepared preforms were determined by the Archimedes principle [15].

Table 1. Chemical composition of aluminium AA 6061 alloy (mass %).

Element	Si	Fe	Cu	Mn	Cr	Zn	Ti	Mg	Al
mass (%)	0.8	0.7	0.4	0.15	0.35	0.25	0.15	1.2	Balance

Table 2. Properties of matrix and reinforcements.

Material	Elastic Modulus (GPa)	Yield Strength (MPa)	Density (kg/m^3)	Poisson's ratio	Coefficient of thermal expansion (CTE) ($\times 10^{-6}/^0C$)
AA 6061	20	80	2700	0.33	23.6
SiC	450	10000	3200	0.17	4.3
Al_2O_3	390	5000	3960	0.25	2.7

Composite material fabrication by the HPDC process

A custom-built squeeze casting apparatus equipped with electrical heating facility (Fig. 1) was set up with a 100-tonne, vertical hydraulic press for direct squeeze casting. A K-type thermocouple connected to a digital thermometer was positioned in the die block to measure temperature changes at the solid-liquid interface. The matrix alloy, AA 6061 ingot was melted in an electrical resistance furnace under an argon protective gas cover. During composite fabrication, the preforms were preheated to 300 ^{0}C and the matrix alloy maintained at 750 ^{0}C was infiltrated into the preforms under an applied pressure of 80 MPa. The pressure holding time for the entire process was 15s. The selection of these parameters is justified by the recommendations of the Authors' [16]. Cooling was accomplished by spraying water at the back of the die cavity wall and the mass flow rate was maintained at 0.2 kg/s. The cooling rate was determined based on the variations in room and die temperatures at 15s interval of time.

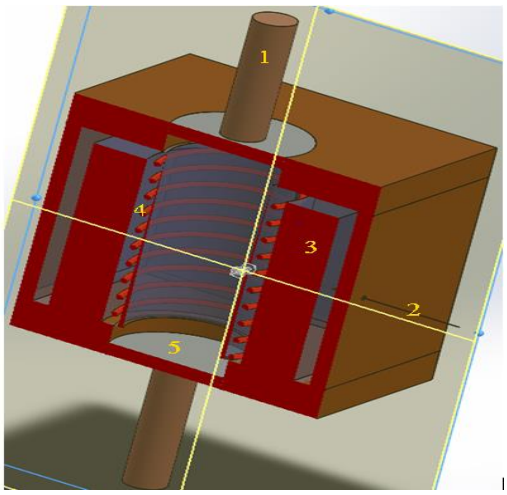

Fig. 1. Schematic of squeeze casting die (1) ram (2) thermocouple probe (3) lagging (4) band heater and (5) ejector rod.

3. Tensile Testing and Characterization of Hybrid Composite

The procedures for the determination of the mechanical properties and the morphological characteristics of the hybrid composite are presented in this section.

3.1. Tensile testing

The tensile properties of the matrix alloy and the squeeze cast hybrid composites were determined using a tensile testing machine (SINTECH 10/GL, MTS, USA) with a crosshead speed of 5.08mm/min equipped with a computer data acquisition system. Test specimens with a rectangular cross section of 25mm gage length, 6mm width and 10mm (Fig. 2) were machined from the cylindrical casts, polished and tested at ambient temperature in accordance with ASTM B557 standard. The normal and the axial axes of the specimens are coincident with the cylindrical casts. The ultimate tensile strength (UTS) and percent elongation which is a measure of the ductility over the gage length, were subsequently determined. An extensometer with a 25.4mm gage length was employed to measure the 0.2% yield strength.

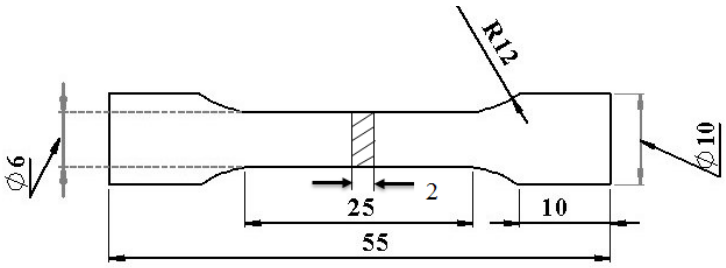

Fig. 2. Tensile test specimen.

3.2. Morphological characteristics

The specimens were mechanically-ground using a silicon carbide impregnated abrasive media of grit sizes ranging between 300-1200 followed by polishing with 1 µm and 0.2 µm Al_2O_3 suspension and 0.05 µm colloidal silica solution. Microstructural analysis was carried out to investigate the morphology of cast specimens using an optical microscope (NKN-4 Nikon Eclipse ME 600) equipped with a GQ camera and scanning electron microscope (LEO 1530).

4. Results and Discussion

The characteristics of the aluminum alloy composite containing 5%, 10% and 20% volume fractions of hybrid-reinforcements were analysed, and the associated solidification processes investigated. The influence of the solidification phenomena on mechanical performance was also presented.

4.1. Hybrid-reinforced composite

The prefabricated preform and the hybrid composite are shown in Fig. 3(a) and (b). The optical micrographs of the unreinforced alloy and hybrid-reinforced composite are shown in Fig. 4. The matrix is shown in Fig. 4(a) while in 4(b,) it is observed that the reinforcement particles are uniformly distributed within the alloy and good bonding is achieved between the reinforcements and the matrix. This could be attributed to the high temperature of processing and the correspondingly high cooling rates. The uniform dispersion of particles would

effectively restrict the dislocation motions through the grain boundaries thereby introducing a strengthening potential in the process [17]. Also, the presence of voids is hardly noticeable in the micrographs indicating that a high densification of the hybrid composites took place in response to the quasi-static application of squeeze pressure during casting [14]. There are no large agglomerations of particles but fine clusters of SiC_p/Al_2O_3 system were present within the primary Al phase as shown in Fig. 4(b) which probably is due to the delay in solidification of the liquid alloy resulting from the effects of the variations in the thermal conductivity of the particles and that of the matrix alloy [18].

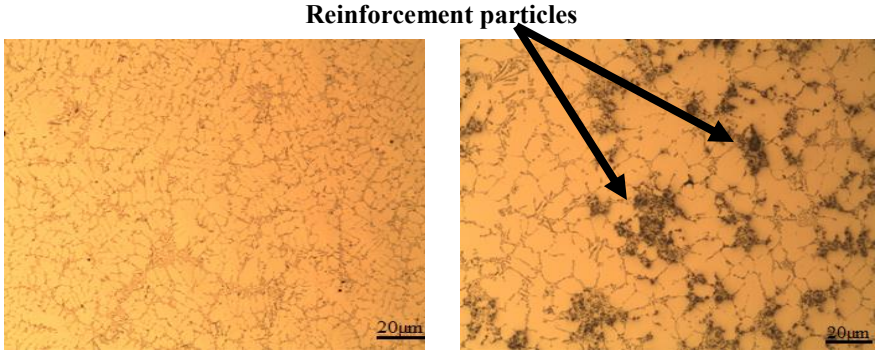

(a) **(b)**

Fig. 3. (a) Prefabricated preform and (b) Hybrid composites.

(a) **(b)**

Fig. 4(a). Optical micrograph of aluminum alloy (b) of hybrid (Al_2O_3+ SiC) reinforced aluminum composite.

4.2. Solidification behavior analysis

The solidification behavior was analysed based on the phase characteristics and effect of solid fraction.

4.2.1. Phase constitution

As shown in Fig. 5(a), the temperature-time analysis of the cooling curves obtained during casting was implemented to determine the solidification behavior

of the cast specimens containing 5%, 10% and 20% volume fraction of reinforcements and the corresponding microstructures are indicated in Figs. 5(b), (c) and (d) respectively.

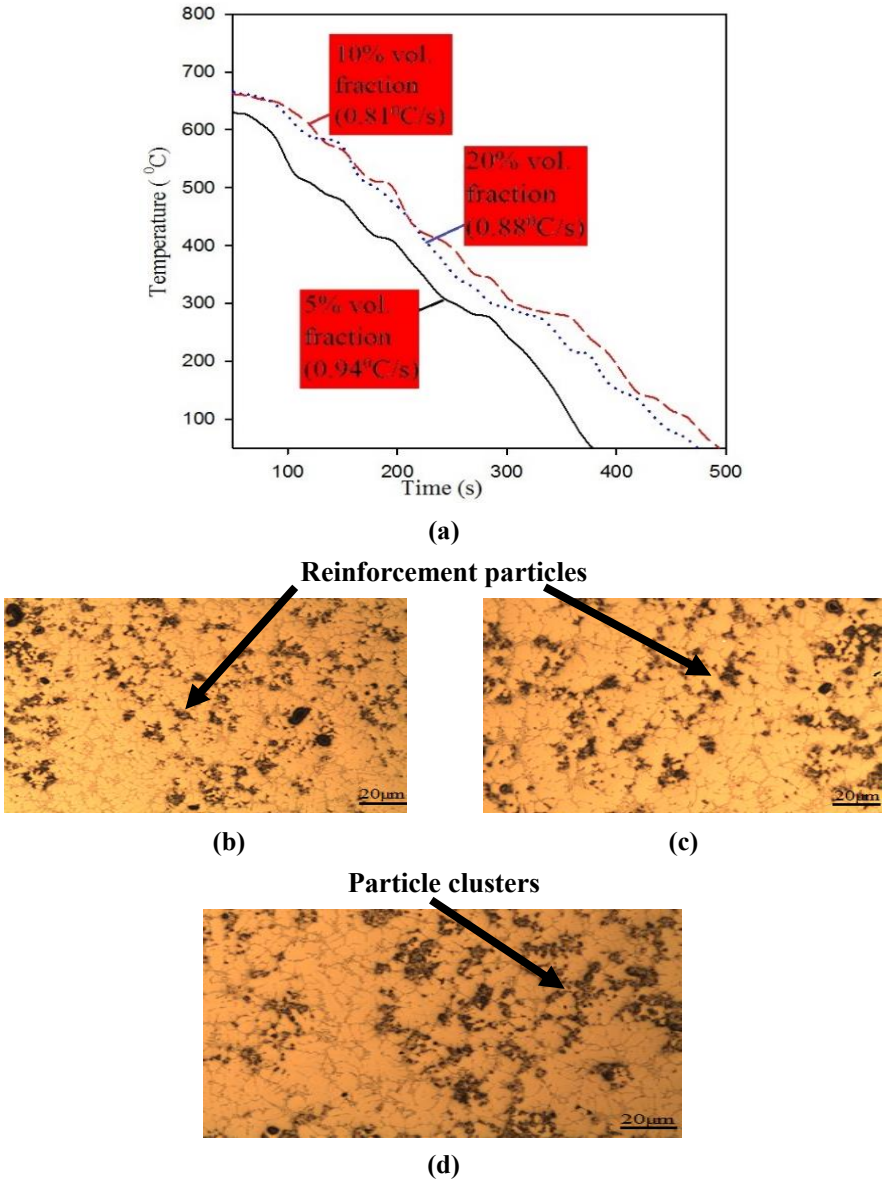

Fig. 5. (a) The cooling curves for Al_2O_3-SiC/AA6061 (b) 5% vol. fraction (0.94 ^{0}C/s) (c) 10% vol. fraction (0.81 ^{0}C/s) (d) 20% vol. fraction (0.88 ^{0}C/s).

In general, the curves are characterized by a very fast region of heat removal, followed by a quasi-linear region indicating a slow but constant cooling process and then a sharp temperature drop until room temperature. According to the

Authors' [11, 13] it is possible to associate with these trends phase formation changes occurring due to the modification of the primary α-Al and eutectic Si particles; and also the nucleation and growth of intermetallic compounds within the solidifying melt during melt-solidification. These scenarios greatly influence the main and post eutectic temperatures which determine the effects of micro constituents on the mechanical behavior of the composite material. Furthermore, the effects of the cooling rate on phase change during the solidification process are very crucial to describing the influence of varying proportions of reinforcement interactions with the solidifying melt. The cooling rate can be associated with the solidification time and it is reflective of the effect of evolution of latent heat during solidification.

The cooling rates shown in Fig. 5 were calculated at the temperature range between 720 and 450 ^{0}C above the linear region for objectivity with respect to the onset of phase reactions. Associated with composite samples containing 5%, 10% and 20% volume fractions of reinforcements are cooling rates of 0.947 ^{0}C/s, 0.81 ^{0}C/s and 0.88 ^{0}C/s with solidification time of 387s, 448s, and 453s respectively. The increased solidification time with increasing reinforcement volume fraction can be attributed to the relative effects of heat rejection by the solidifying alloy due to its latent heat, resulting in an increase in the temperature of the particle clusters [12] which retards the velocity of the solidification front.

By taking the first derivative of these curves and fitting with a second degree polynomial, the determination of critical solidification characteristics was facilitated [19]. It was observed that by plotting these derivatives as a function of time (i.e. dT/dt-t), the T-t curves transformed into sharp peaks on the dT/dt-t curves, indicating the point at which the onset of phase reactions took place during solidification due to the dissipation of latent heat from the micro-constituents. The phenomenon of phase transformations is contingent on the solidification time and influence of characteristic temperatures (the nucleation, the eutectic and the post eutectic temperatures) that can be obtained from the curves, and the ensuing inherent fluctuations, provide a platform for comparing the kinetics of solidification of the hybrid-reinforced composite with respect to varying volume fraction of reinforcements.

From Fig. 6, three/four notable peaks were identified corresponding to three/four phase transformations. The first phase which is nucleation (Al: 5%, 10%. 20%) is associated with the formation and growth of α-Al dendrites, the second phase is attributed to the growth of eutectic silicon (Eu-Si: 5%, 10%, 20%) and the third, is the post eutectic reaction phase concerned with the formation of intermetallic compounds (I: 5%, 10%, 20%). As observed, the composite sample containing 5% volume fraction of reinforcements presented higher peaks associated with nucleation as compared with the samples containing 10% and 20% volume fraction of reinforcements this suggests that there was a higher rate of latent heat release during solidification due to the faster distribution of solidified particles in the melt caused by the strong convective effects introduced at the onset of cooling.

However, at this stage, the difference between the 10% and 20% samples was not quite significant. Hence, the drastic drop in temperature at the onset of nucleation for the composite sample with 5% vol. fraction of reinforcement may also be attributed to the extent to which there is a reduction in the temperature for

liquidus in equilibrium for the matrix material (Al-Si) system [13]. Subsequently, by investigating the Eu-Si peaks, it is evident that the 10% peak is only slightly higher than the 5% and 20% peaks both of which were almost at par in shape suggesting that there were no significant variations in the temperatures at which the clustering of silicon atoms occurred prior to nucleation and growth of eutectic silicon. Hence, the precipitation temperatures of the second phase is fairly uniform for all the samples which follows that the rate of heat extraction is somewhat equal to the latent heat released for nucleation and growth of the eutectic nuclei. The extent of modification of the primary α-Al dendrites and eutectic Si particles with respect to varying volume fractions of reinforcements now explicitly depend on the solidification rate in this region.

Furthermore, the format ion mechanism of intermetallic compounds which is a strong feature in the solidification process of aluminum composites suggests that the latter part of the solidification process is strongly influenced by the volume fraction of reinforcements as indicated by the variations in the intensities and shapes of the third peaks from the cooling curves as the growth of eutectic micro constituents occur at varying post eutectic temperatures. For the sample with 10% volume fraction of reinforcement, the peak was the highest, followed by the 5% and 20% peaks and the extent of variations in these maxima is also significant in that order. The trend indicates that significant variations in temperature gradients occurred towards the end of solidification process.

This is evident by the broader peak corresponding to the sample with 5% vol. fraction indicating that solidification is completed at a lower temperature with a degree of greater recalescence, while the sharper peaks in relation to the 10% and 20% vol. fraction suggest that the end of solidification proceeded at fairly constant temperatures. The temperatures at the onset of the reactions at this stage are sensitive to increases in the volume fraction of reinforcements.

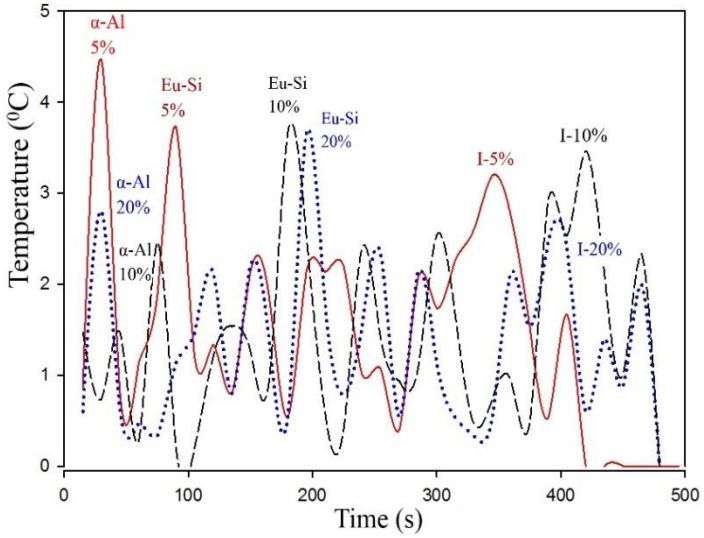

Fig. 6. First derivative curves of cooling profile for the particle reinforced Al_2O_3-SiC/AA6061 at 5%, 10% and 20% volume fractions.

4.2.2. Solid fraction

The solidification phenomena is also strongly influenced by the 'fraction of solid' property which is an important characteristic describing the thermal events at any temperature/time domain during phase transformation. To determine this property, the Newtonian method [11] which assumes that no thermal gradients exist within the casting was applied. In this particular case, a baseline curve which gives the time evolution of the cooling rate curve with reference to no phase transformation is required. This is computed by fitting a third-order polynomial to a set of data from the first derivative curve chosen before the liquids and after solidus temperature of the alloy. The baseline equation is expressed by Eq. (1).

$$\left(\frac{dT}{dt}\right)_{bl} = A + BT + CT^2 + DT^3 \tag{1}$$

According to the heat balance equation during solidification, the solid fraction parameter f_s can be expressed by Eq. (2)

$$f_s = \frac{\int_{t_1}^{t}\left[\left(\frac{dT}{dt}\right)_{cc} - \left(\frac{dT}{dt}\right)_{bl}\right]dt}{\int_{t_1}^{t_s}\left[\left(\frac{dT}{dt}\right)_{cc} - \left(\frac{dT}{dt}\right)_{bl}\right]dt} \tag{2}$$

where, cc and bl refer to the cooling and the baseline curves respectively. The begining and end of solidification are t_l and t_s respectively, i.e., the time at liquidus and solidus. The cooling curves provide the relationship between the alloy temperature T and solidification time t from where it was possible to obtain the solid fraction at a given temperature T from the calculated t-f_s relationship.

From the resulting T-fs curves that are plotted in Fig. 7. It was observed in general, that the solid fraction increases rapidly at the onset of solidification, it then slows down and continues to increase gradually over a large temperature range. By associating this trend with increasing volume fraction of reinforcements, it is noticed that solid fraction at the eutectic temperature range remains fairly constant, indicating a longer time for solidification due to the effect of latent heat evolution which allows the eutectic cells to grow larger during this period [11]. At the intermetallic regions, the solid fraction increase is significant; indicating that the end of solidification process which is critical to grain boundary strengthening is sensitive to the influence of reinforcement particle additions during solidification processing.

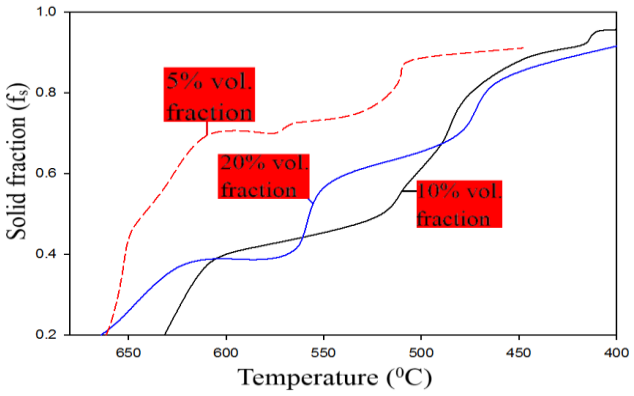

Fig. 7. T-f_s curves for the particle reinforced Al_2O_3-SiC/AA6061 at 5%, 10% and 20% volume fractions.

Furthermore, the solid fraction governs the effects of cooling rates; and since higher cooling rates are associated with increasing dendritic growth, it is logical to state that the dendritic growth rates at 10% volume fraction of reinforcement is a most prominent feature based on the observations from the initial solidification phase with respect to the influence of 5%, 10% and 20% volume fractions of reinforcements within the alloy matrix.

4.3. Mechanical properties of the hybrid composite

The variations in the mechanical properties of the hybrid composite are shown along with that of the matrix (AA 6061 alloy) in Table 3. The ultimate tensile (UTS) and yield (YS) strengths of the hybrid composite are significantly higher than that of the matrix but with a reduction in percent elongation. At 5% volume fraction of reinforcement additions, the elastic modulus, YS and UTS increased by (36%), (11%) and (4%) respectively over that of the unreinforced alloy with a reduction of (7.7%) in percent elongation. At 10% volume fraction of reinforcements there is a further slight reduction in percent elongation by (4%) but the elastic modulus increased by (5%) while the YS and UTS increased tremendously by (14.4%) and (7%) respectively when compared with the performance of the matrix alloy. This phenomenon could be attributed to the strengthening effect of the hard reinforcement particles and their homogenous dispersion within the matrix could have introduced a higher strain to inhibit grain growth requiring a larger driving force for nucleation at the grain boundaries.

Table 3. Mechanical properties of Al_2O_3-SiC/AA6061.

Sample	Elastic Modulus (GPa)	Yield Strength (MPa)	Ultimate Tensile Strength (MPa)	Percent elongation
Unreinforced alloy	69	114	188	8.6
5% vol. fraction	93.8	127	197	8.0
10% vol. fraction	97.2	143	209	7.6
20% vol. fraction	98.7	149	214	5.1

Furthermore, the higher UTS of the composite may also be due to the formation of the intermetallic phases such as the Al strengthening phases which introduces substantial effect of dispersion hardening in the course of decomposition of supersaturated solid solutions in the matrix alloy composite [20]. The increase in elastic moduli may be attributed to the high stiffness of the reinforcement particles which act as stress concentrators, thereby locally increasing and extending the plastic deformation process. However, at 20% volume fraction of reinforcements, mechanical performance was only marginal, the elastic modulus only increased by (2%), while the YS and UTS increased by (5.3%) and (2.8%) respectively. Accompanied by this, is a significant dip in elongation by (28.7%). The reduction in percent elongation and poor

improvement in elastic modulus may be attributed to particle fracture and diminishing interfacial strength as the volume fractions increased from 0-20% and the ductile matrix content reduces. In general however, there is a correspondence between ductility loss with reference to increasing volume fraction of reinforcements, an effect that could be attributed to poor strain hardening behavior or the progressive development of plastic instabilities with straining during deformation. At any rate, the enhanced mechanical properties of the hybrid composite as compared with the unreinforced alloy suggest that particle strengthening from the Al_2O_3-SiC reinforcement system have a beneficial effect on the aluminum alloy composite.

From the melt-solidification standpoint, higher cooling rates were associated with lower volume fraction of reinforcements and higher release of latent heat. The enhanced solidification front resulting from this effect facilitated the infiltration of the matrix alloy within the preform ceramic structure thus providing necessary conditions to raise the internal stresses between the reinforcements and the matrix during deformation under tensile loading leading to a higher resistance to slip by the matrix. However, the improvements in mechanical properties become less significant as the solidification time increases with increase in volume fraction of reinforcements. From the foregoing, it is reasonable to state that a controlled solidification process can enhance the load bearing capacity of the hard particles within the matrix alloy, while the effect of strain mismatch between the matrix alloy and the reinforcement particles during deformation could also have contributed to the improved strengths of the hybrid composites [21].

4.4. Fracture behavior

The fracture characteristics of the hybrid reinforced composites are as shown in Figs. 8-11 and they represent the morphology of the composite material containing 0%, 5%, 10% and 20% volume fraction of reinforcements. The effects of particle strengthening is observed in general, and it follows that during tensile loading, the flow of deformation proceeded through the particles located at the grain boundaries leading to intergranular-like fracture when the critical deformation stress was reached. During solidification processing, strain fields are generated around the hard particles due to the variations in the coefficient of thermal expansion between the particles and aluminum alloy. Hence, the dominant fracture initiation mode is associated with strain localization effects at the sharp edges of the reinforcement particles [18] and also due to restrictions to the continuity of dendritic cell boundaries by the presence of eutectic secondary phase elements. These coupled scenarios may account for the enhanced ultimate tensile strengths and simultaneously a reduction in ductility at the microscopic level.

Furthermore, features of mixed mode cleaveage-like brittle and intragranular fracture mechanisms can be seen as the reinforcement volume fraction increases from 10-20% and they are characterized by small sized dimples which are features associated with weak interfacial bonding. The formation of dimples and propagating cracks caused by microvoids initiating at the boundary regions also accounts for the variations in the yield strength and the reduction of percent elongation or ductility of the composite material as the volume fraction of reinforcements is increased progressively. Nonetheless, the prevailing mode of failure still suggests that the interfacial bonding strength between the

reinforcements was strong enough to facilitate the load bearing capacity of the particles since the failure of the matrix would only have to occur by the coalescence of microvoids [18].

From the foregoing, it can be stated concerning the composite material with 5% volume fractions of reinforcements, that the presence of a clear interface and better bonding characteristics delayed the detachment of the particles from the matrix, a phenome-non that improved the UTS of the composite material significantly. At 10% volume fraction of reinforcements, the intensity of the interactions between dislocations and the particles increased favorably which consequently increased the strain to failure at the crack tip with an enhancement in mechanical properties. But as the volume fraction was increased to 20%, the influence of particle cracking be-comes critical and the interface is weakened with a loss of ductility and a reduction in mechanical properties.

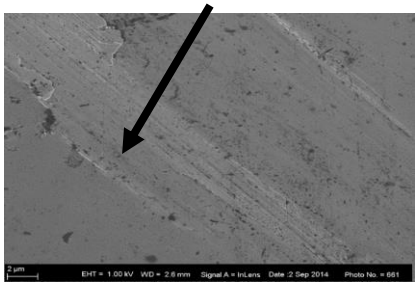

Fig. 8. Unreinforced alloy.

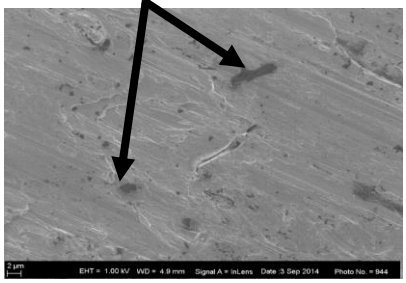

Fig. 9. 5% vol. fraction Al_2O_3SiC/AA6061

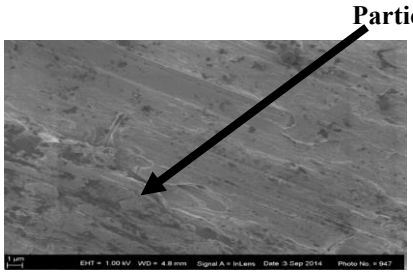

Fig. 10. 10% vol. fraction Al_2O_3-SiC/AA6061.

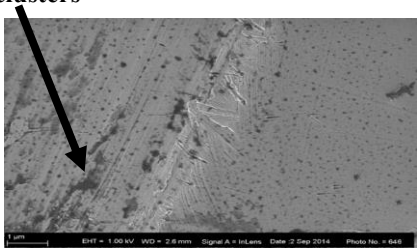

Fig. 11. 20% vol. fraction Al_2O_3-SiC/AA6061.

5. Conclusions

The solidification behaviour of hybrid reinforced (Al_2O_3-SiC) aluminum AA 6061 has been investigated and the following are the inferences drawn.

- The high pressure die casting (HPDC) process was successfully implemented for the synthesis of aluminum alloy AA6061 with 5%, 10% and 20% volume fraction of hybrid (Al_2O_3-SiC) particle reinforcements.

- The solidification mechanism in the HPDC process is sensitive to variations in the volume fraction of reinforcements as indicated by the phase reactions. For the sample with 5% volume fraction of reinforcement, the variations in temperature at the beginning and the end of the solidification were significant while for samples with 10% and 20% volume fraction of reinforcements, this process occurred at fairly constant temperatures.
- The solidification time increased progressively with increasing volume fraction of reinforcements as the cooling rate reduces. The solidification front is retarded due to the slower release of latent heat with increasing reinforcement concentration.
- The elastic modulus, yield and tensile strengths were enhanced as the volume fraction of reinforcements increases, with an associated decline in percent elongation. Nonetheless, there were no significant improvements in these properties as the solidification time increases.

References

1. Miracle, D.B. (2005). Material matrix composites-from science to technology significance. *Composite Science and Technology*, 65(15-16), 2526- 2540.
2. Bozic, D.; Dimic, B.; Dimic, O.; Stasic, J.; and Rajkovic, V. (2010). Influence of SiC particles distribution on mechanical properties and fracture of DRA alloy. *Materials & Design*, 31(1), 134-141.
3. Chen, C.-Y.; and Chao, C.-G. (2000). Effect of particle size distribution on the properties of high-volume-fraction Si*Cp*-Al based composites. *Metallurgical and Materials Transactions A*, 31(9), 2351-2359.
4. Thünemann, M.; Beffort, O.; Kleiner, S.; and Vogt, U. (2007). Alumnium matrix composites based on preceramic-polymer-bonded SiC preforms. *Journal of Composite Science and Technology*, 67(11-12), 2377-2383.
5. Bertelli, F.; Brito, C.; Meza, E.S.; Cheung, N.; and Garcia, A. (2012). Inward and outward solidification of cylindrical casting: The role of the metal/mold heat transfer coefficient. *Materials Chemistry and Physics,* 136(2-3), 545-554.
6. Böyük, U.; Maraşlı, N.; Çadırlı, E.; Kaya, H.; Keşlioğlu, K. (2012). Variation of microhardness with solidification parameters and electrical resistivity with temperature for Al-Cu-Ag eutectic alloy. *Current Applied Physics*, 12(1), 7-10.
7. Liu, L.; Huang, T.; Qu, M.; Liu, G.; Zhang, J.; and Fu, H. (2010). High thermal gradient directional solidification and application in the processing of nickel-based superalloys. *Journal of Materials Processing Technology,* 210(1), 159-165.
8. Chen, R.; Shi, Y.-F.; Xu, Q.-Y.; and Liu. B.-C. (2014). Effect of cooling rate on solidification parameters and microstructure of Al-7Si-0.3Mg-0.15Fe alloy. *Transactions of Nonferrous Metals Society of China*, 24(6)*,* 1645-1657.
9. Hosseni, V.A.; Shabestari, S.G.; and Gholizadeh, R. (2013). Study on the effect of cooling rate on the solidification parameters, microstructure and mechanical properties of LM 13 alloy using cooling curve thermal analy- sis technique. *Materials & Design,* 50, 7-14.
10. Fan, J.; Li, X.; Su, Y.; Guo, J.; and Fu, H. (2010). Dependency of micro-hardness on solidification processing parameters and microstructure

characteristics in the directional solidified Ti-46Al-0.5N-0.5Si alloy. *Journal of Alloys and Compounds*, 504(1), 60-64.

11. Li, J.; Chen, R.; Ma, Y.; and Ke, W. (2014). Computer-aided cooling curve thermal analysis and characterization of Mg-Gd-Y-Zr system alloys. *Thermochimica Acta,* 590, 232-241.
12. Baez, J.C.; Gonzalez, C.; Chavez, M.R.; Castro, M.; and Juarez. (2004). Fourier thermal analysis of the solidification kinetics in A356/SiCp cast composites. *Journal of Materials Processing Technology,* 153-154, 531-536.
13. Farahany, S.; Nordin, N.A.; Quardjini, A.; Abu Bakar, T.; Hamzah, E.; Idris, M.H.; and Hekmat-Ardakan, A. (2014). The sequence of intermetallic formation and solidification pathway of an Al-13Mg-7Si-2Cu in-situ composite. *Materials Characterization,* 98, 119-129.
14. Amin, K.; and Mufti, N.A. (2012). Investigating cooling curve profile and microstructure of a squeeze cast Al-4% Cu alloy. *Journal of Materials Processing Technology,* 212(8), 1631-1639.
15. Fan, G.H.; Geng, L.; Lai, Z.H.; and Wang, G.S. (2009). Preparation and Properties of hybrid composite based on ($BaPbO_3$ + $Al_{18}B_4O_{33}$)/6061 Al system. *Journal of Alloys and Compounds*, 482(1-2), 512-515.
16. Vijian, P.; and Arunachalam, V.P. (2007). Modelling and multi-objective optimization of LM 24 aluminum alloy squeeze cast process parameter using genetic algorithm. *Journal of Materials Processing Technology*, 186(1-3), 82-86.
17. Wong, W.L.E.; Gupta, M.; and Lim, C.Y.H. (2006). Enhancing mechanical properties of pure aluminum using hybrid reinforcement methodology. *Journal of Materials Science and Engineering A*, 423(1-2), 148-152.
18. Rajmohan, T.; Palanikumar, K.; and Ranranathan, S. (2013). Evaluation of mechanical and wear properties of hybrid aluminum matrix composites. *Journal of Transactions of Nonferrous Metals Society of China*, 23(9), 2509-2517.
19. Canales, A.; Talamantes-Silva, J.; Gloria, D.; Valtierra, S.; and Colas, R. (2010). Thermal analysis during solidification of cast Al-Si alloys. *Thermochimica Acta*, 510(1-2), 82-87.
20. Ashok Kumar, B.; and Murugan, N. (2012). Metallurgical and mechanical characterization of stir cast AA6061-T6-AINp composite. *Materials & Design*, 40, 52-58.
21. Xu, N.; and Zong, B.Y. (2008). Stress in particulate reinforcement and overall stress response on aluminum alloy matrix composites during straining by analytical and numerical modeling. *Journal of Computational Materials Science*, 43(4), 1094-1100.